ELECTRONIC SUPPLEMENTARY INFORMATION (ESI)

Self-Organization towards Complex Multi-Fold Meso-Helixes in the Structures of Wells-Dawson Polyoxometalate Based Hybrid Materials for Lithium-Ion Batteries

Mengting Li,[a] Lina Cong,[a] Jiao Zhao,[a] Tiantian Zheng,[a] Rui Tian,[a] and Jingquan Sha,[b]*
Zhongmin Su[a] and Xinlong Wang [a]*

[a.] *Address here. Institute of Functional Material Chemistry, National & Local United Engineering Laboratory for Power Batteries, Northeast Normal University, Changchun, 130024 Jilin, People's Republic of China.*

[b.] *Department of Chemistry and Chemical Engineering, Jining University, Qufu, 273155, China.*

*E-mail: wangxl824@nenu.edu.cn and shajq2002@126.com

Synthesis of $[Ag_{26}(Trz)_{16}(OH)_4][P_2W_{18}O_{62}]$ (1) The mixture of $K_6P_2W_{18}O_{62}$ (100 mg), $AgNO_3$ (100 mg), Trz (15 mg) was dispersed in 8 mL of distilled H_2O by stirring for 1 h at ambient temperature. And the pH value of mixture was adjusted to 2.4 and heated at 180 °C in Teflon-lined reactor for 3 days. Then we collected the brown blocks at ambient temperature. Yield: 30% based on Ag. Anal. Calcd for $C_{32}H_{36}N_{48}Ag_{26}P_2W_{18}O_{66}$ (8324.55): C 4.62, H 0.43, N 8.08%; Found C 4.64, H 0.40, N 8.1%.

Synthesis of $Na[Ag_{16}(Trz)_9(H_2O)_4][P_2W_{18}O_{62}]\cdot H_2O$ (2) The synthesis process of **2** is similar with 1 except for the pH value of mixture was adjusted to 1.7. Then we collected the dark brown blocks at ambient temperature and washed with water for few times. Yield: 23% based on Ag. Anal. Calcd for $C_{18}H_{28}N_{27}Ag_{16}P_2W_{18}O_{67}Na$ (6814.51): C 3.17, H 0.41, N 5.55%; Found C 3.18, H 0.40, N 5.57%.

Materials and Measurements. Powder X-ray diffraction (PXRD) patterns, FT-IR spectra, thermogravimetric analysis (TGA) and elemental analyses were measured on Siemens D5005 diffractometer (Cu-Kα (λ = 1.5418 Å) radiation), Alpha Centaurt FT/IR spectrophotometer (KBr pellets), Perkin-Elmer TG-7 analyzer and Perkin-Elmer 240C elemental analyzer, respectively.

X-ray Crystallographic Measurements. Bruker SMART-CCD diffractometer with monochromatic Mo-Kα radiation (λ = 0.71069 Å) was used for collecting the crystallographic data of **1** and **2** at 293 K. Absorption corrections were applied using multiscan technique and conducted by using the SADABS program.[1] In order to solve and refine the structures of title compounds, we emploied the direct method and full matrix least-squares with the *SHELXTL*.[2] We used the anisotropically operation to refine all the atoms except for hydrogen atoms.

Battery analyses. We used **1** and **2** as the anode materials to study the electrochemical perfomance of LIBs, $(NBu_4)_6[P_2W_{18}O_{62}]$ and graphite as reference anodes material. By mixing title compound (70 wt%), Super-P carbon (20 wt%), and poly(vinylidene fluoride) (10 wt%) we get the anodes. Then added N-methyl-2-pyrrolidinone (NMP) to the mixture to form a paste with appropriate viscosity. Then the paste was coated on pure Cu foil mildly and vacuum dried at 50 °C for 24 h. The active anode material loading mass of on each electrode disk is about 2 mg cm^{-2}. Button cell was assembled with the working electrode, Li counter electrode, and 1.0 M $LiPF_6$ in ethylene carbonate (EC)/diethyl carbonate (DEC) (1:1 v/v) as the electrolyte. We used the LAND CT2001A instrument (Wuhan, China) and electrochemical workstation (Princeton Applied Research, Germany) to record the circulation measurements, Cyclic voltammetry (CV) and electrochemical impedance spectroscopy (EIS) of batteries at constant ambient temperature, respectively.

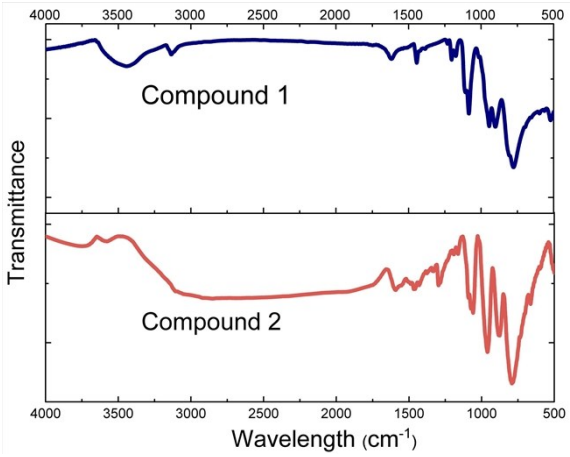

Figure S1. FT-IR spectra of **1** and **2**.

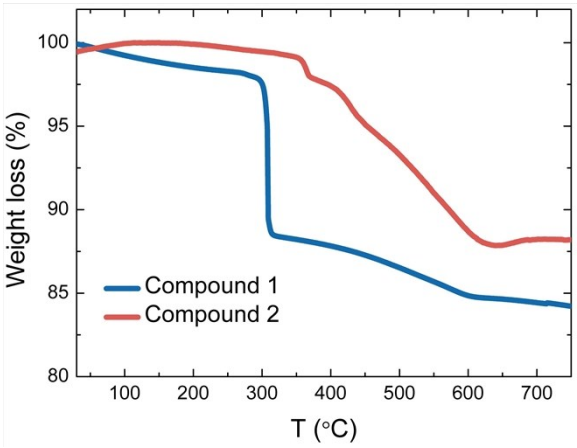

Figure S2. The TGA curve of **1** and **2**.

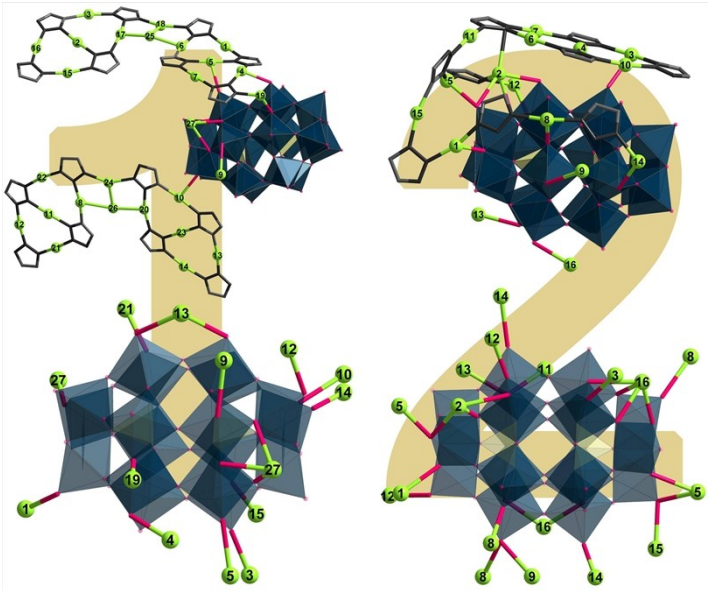

Figure S3. Ball/stick/polyhedral view of the crystallographic unitand the coordination pattern of the P2W18polyanion of compound **1** (left), and **2** (right). All of the hydrogen atoms and crystal water molecules were omitted for clarity.

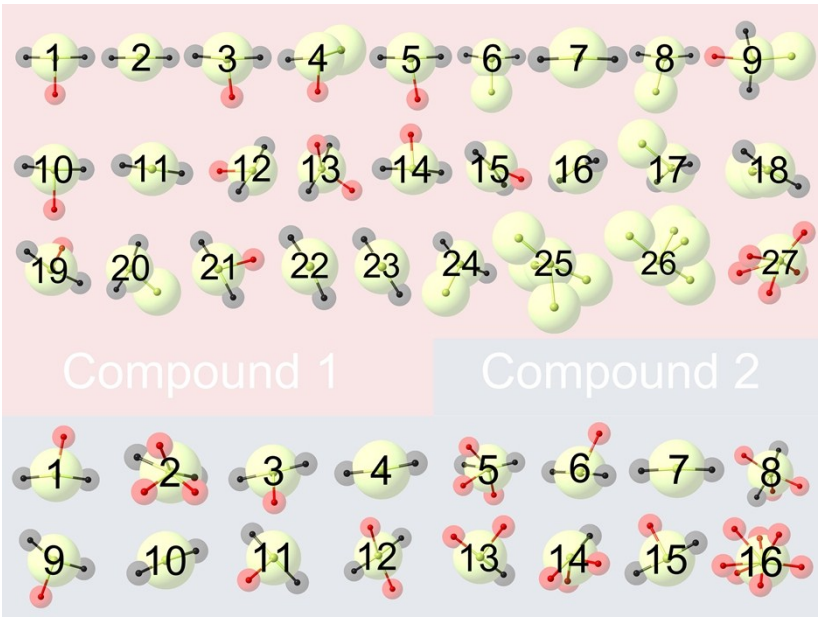

Figure S4. Schematic illumination of the coordination modes of Ag^{+} ions of **1** and **2**.

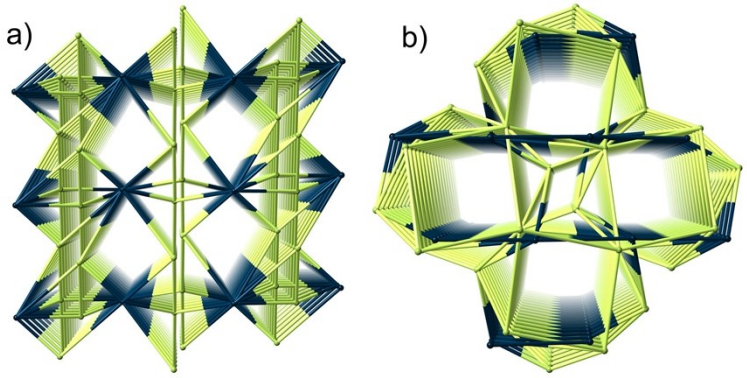

Figure S5. Schematic illustration of the topology of a) **1** and b) **2** along *a* axis. The dark blue nodes represent P_2W_{18} polyanions, and the luminous green nodes symbolize Ag^{+} ions.

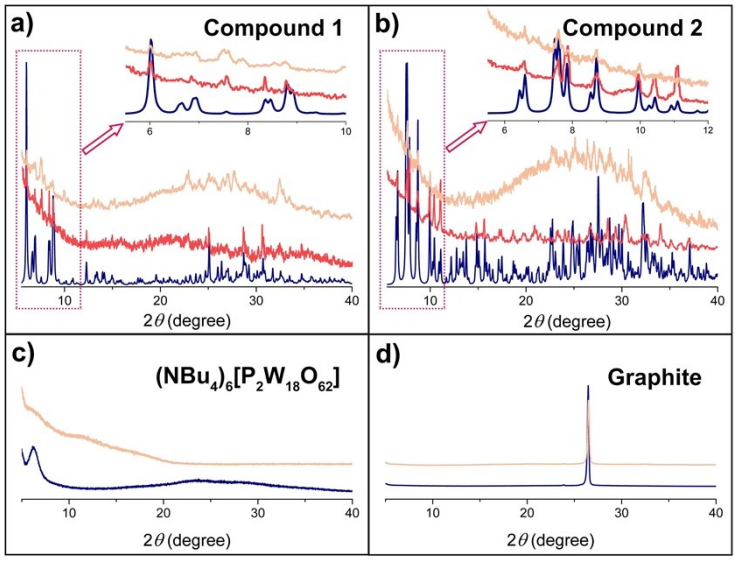

Figure S6. The PXRD patterns of a) simulated (blue), experimental (red) of crystal **1** and **1** as anode after cycling (yellow); b) simulated (blue), experimental (red) of crystal **2** and **2** as anode after cycling (yellow); c) and d) $(NBu_4)_6[P_2W_{18}O_{62}]$ and commercial graphite as reference anodes before (blue) and after (yellow) cycling.

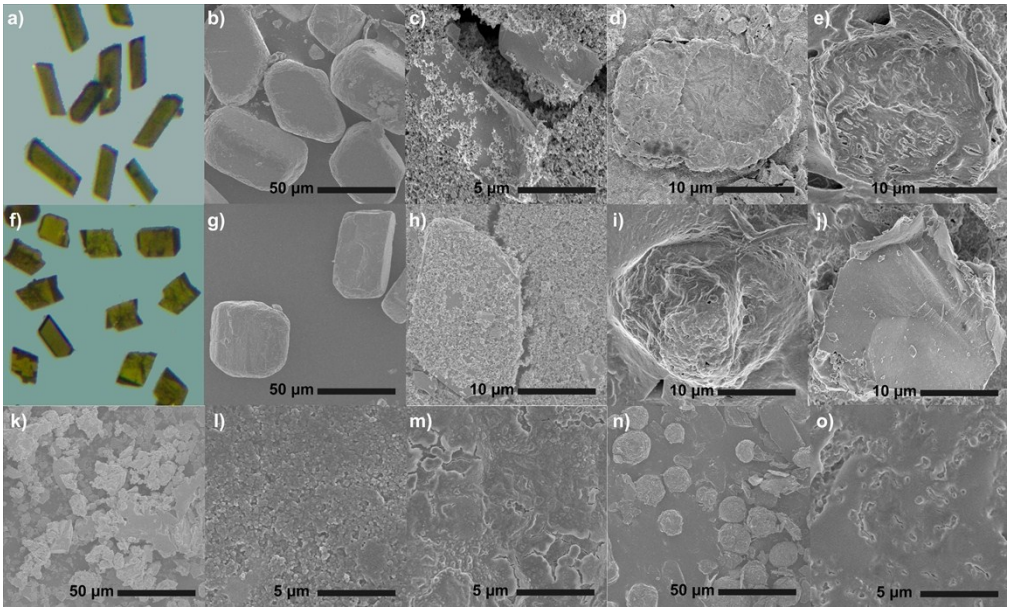

Figure S7. Photos of single crystals of a) **1** and f) **2**; SEM images of b) single crystals of **1**; c) **1** as anode befor cycling; d) and e) **1** as anode after cycling; g) single crystals of **2**; h) **2** as anode before cycling; i) and j) **2** as anode after cycling; k) amorphous powder of $(NBu_4)_6[P_2W_{18}O_{62}]$; l) $(NBu_4)_6[P_2W_{18}O_{62}]$ as reference anode before cycling; m) $(NBu_4)_6[P_2W_{18}O_{62}]$ as reference anode after cycling; n) graphite as reference anode before cycling and o) graphite as reference anode after cycling performance.

Calculation of the theoretical capacity. According to the description reported by Cronin *et al*,[13] we calculated the theoretical capacities of **1** and **2**. The first discharge capacities of the **1** and **2** are 1077 mA h g^{-1} and 1094 mA h g^{-1}, respectively. When charging back to 2.5 V, a reversible charging-discharging capacities of 550 mA h g^{-1} and 600 mA h g^{-1} are obtained for **1** and **2**. According to the equation:

$$Q = \frac{nF}{3.6M_W} = \frac{96500n}{3.6M_W}$$

where *Q* is the reversible charging-discharging capacity, *n* is the number of electrons passed during the redox reaction, and *M*w is the molecular weight of compounds (**1**=8324.55 g mol^{-1} and **2**=6814.51 g mol^{-1}), the translocation of each Li^+ to/from the POM cluster contributes the capacity of around 3.22mA h g^{-1} for **1** and 3.93mA h g^{-1} for **2**. As a result, we calculate that about 335 W^{VI} centers (1077/3.22) for **1** and 297 W^{IV} centers (1094/3.93) for **2** are electrochemically reduced to W^{V} during the first discharging process, and that 170.8 W^{VI} centers (550/3.22) for **1** and 152.6 W^{IV} centers (600/3.93) for **2** undergo electrochemical oxidation during the subsequent charging process (and in the charge-discharge processes thereafter). The theoretical specific capacities for **1** and **2** within this voltage window can then be calculated by taking *n* to be 171 for **1** and 153 for **2** (the next nearest integer number of electrons), and feeding this number back into the equation above to find the theoretical specific capacities for **1** of 551 mA h g^{-1} and **2** of 602 mA h g^{-1}.

Table S1. The fitting errors of the simulated equivalent circuit of 1 and 2 anodes.

	Compound 1	Fitting Error (%)	Compound 2	Fitting Error (%)
R_e (Ω)	3.333	1.7905	3.358	2.1476
R_f (Ω)	45.71	2.9085	57.78	1.051
R_{ct} (Ω)	125.6	19.112	147.2	21.008
Sum (Ω)	174.643	-	208.338	-

Table S2. Crystal data and structure refinement for compounds 1 and 2.

Compound reference	**1**	**2**
Chemical formula	$C_{32}H_{36}N_{48}Ag_{26}P_2W_{18}O_{66}$	$C_{18}H_{28}N_{27}Ag_{16}P_2W_{18}O_{67}Na$
Formula Mass	8324.55	6814.51
Crystal system	Triclinic	Monoclinic
a/Å	15.025(5)	16.951(5)
b/Å	15.036(5)	23.303(5)
c/Å	28.658(5)	27.845(5)
α/°	85.652(5)	90.00
β/°	86.867(5)	125.992(11)
γ/°	77.497(5)	90.00
Unit cell volume/Å3	6298(3)	8899(4)
Temperature/K	293(2)	293(2)
Space group	*P-1*	*P2(1)/c*
No. of formula units per unit cell, *Z*	2	4
Final R_1 values ($I > 2\sigma(I)$)	0.0633	0.0974
Final $wR(F^2)$ values ($I > 2\sigma(I)$)	0.1539	0.2484
Final R_1 values (all data)	0.1069	0.1804
Final $wR(F^2)$ values (all data)	0.1767	0.3047
Goodness of fit on F^2	0.992	1.058
CCDC no.	1509077	1509078

[a] $R_1 = \sum \left| |F_o| - |F_c| \right| / \sum |F_o|$. [b] $wR_2 = \{\sum[w(F_o^2 - F_c^2)^2] / \sum[w(F_o^2)^2]\}^{1/2}$

Table S3. Selected bonds lengths (Å) and angles (°) for compound 1.

Ag(1)-N(28)	2.05(2)	Ag(1)-N(9)#2	2.10(2)
Ag(2)-N(34)	2.07(2)	Ag(2)-N(1)	2.090(19)
Ag(3)-N(15)#3	2.09(2)	Ag(3)-N(3)#4	2.13(2)
Ag(4)-N(5)	2.213(19)	Ag(4)-N(30)#5	2.23(2)
Ag(5)-N(29)	2.03(2)	Ag(5)-N(48)#6	2.03(2)
Ag(6)-N(8)	2.17(2)	Ag(6)-N(47)#7	2.17(2)
Ag(7)-N(46)	2.10(2)	Ag(7)-N(6)	2.13(2)
Ag(8)-N(10)	2.13(2)	Ag(8)-N(44)#8	2.131(19)
Ag(9)-N(25)	2.14(2)	Ag(9)-N(32)	2.16(2)
Ag(10)-N(38)	2.10(2)	Ag(10)-N(41)#9	2.11(2)
Ag(11)-N(23)	2.07(2)	Ag(11)-N(45)#5	2.09(2)
Ag(12)-N(22)	2.11(2)	Ag(12)-N(26)	2.11(2)
Ag(13)-N(31)	2.10(2)	Ag(13)-N(37)#8	2.15(2)
Ag(14)-N(33)#9	2.07(2)	Ag(14)-N(21)#3	2.12(2)
Ag(16)-N(16)	2.09(2)	Ag(16)-N(2)	2.12(2)
Ag(17)-N(13)	2.159(19)	Ag(17)-N(36)#10	2.16(2)
Ag(18)-N(7)	2.17(2)	Ag(18)-N(14)	2.19(2)
Ag(19)-N(17)	2.11(2)	Ag(19)-N(4)	2.13(2)
Ag(20)-N(42)#11	2.15(2)	Ag(20)-N(19)	2.16(2)
Ag(21)-N(43)	2.104(17)	Ag(21)-N(27)#6	2.12(2)
Ag(22)-N(12)	2.129(19)	Ag(22)-N(24)#12	2.13(2)
Ag(23)-N(39)#12	2.079(18)	Ag(23)-N(20)	2.09(2)
Ag(24)-N(40)	2.19(2)	Ag(24)-N(11)	2.20(2)
O(86)-Ag(14)	2.569(15)	O(69)-Ag(27)#6	2.407(17)
Ag(27)-O(69)#5	2.407(17)	O(86)-Ag(14)	2.569(15)
O(70)-Ag(21)	2.566(18)	O(75)-Ag(3)	2.493(14)
O(81)-Ag(1)#1	2.580(17)	N(27)#6-Ag(21)-O(70)	101.9(7)
N(28)-Ag(1)-N(9)#2	174.5(9)	N(34)-Ag(2)-N(1)	176.1(8)
N(15)#3-Ag(3)-N(3)#4	170.3(8)	N(5)-Ag(4)-N(30)#5	153.6(7)
N(29)-Ag(5)-N(48)#6	174.8(8)	N(8)-Ag(6)-N(47)#7	165.7(8)
N(46)-Ag(7)-N(6)	175.1(9)	N(10)-Ag(8)-N(44)#8	166.2(7)
N(25)-Ag(9)-N(32)	155.9(8)	N(33)#9-Ag(14)-O(86)	87.8(6)
N(21)#3-Ag(14)-O(86)	94.7(7)	N(13)-Ag(17)-N(36)#10	159.9(8)
N(7)-Ag(18)-N(14)	156.0(8)	N(17)-Ag(19)-N(4)	163.1(8)

Symmetry transformations used to generate equivalent atoms: #1 = -x+1,-y+2,-z+2; #2 =-x+1,-y,-z+2; #3 = x-1,y+1,z; #4 = -x+1,-y+1,-z+2; #5 =x,y-1,z; #6 = x,y+1,z; #7 = -x+1,-y-1,-z+2; #8 =-x+1,-y+2,-z+1; #9 = x-1,y,z; #10 = -x+2,-y,-z+2; #11 =-x+2,-y+1,-z+1; #12= -x+1,-y+1,-z+1; #13 = x+1,y-1,z; #14 =x+1,y,z.

Table S4. Selected bonds lengths (Å) and angles (°) for compound 2.

N(22)-Ag(15)-O(41)#6	95.3(12)	Ag(1)-N(7)	2.11(4)
Ag(1)-N(27)#2	2.12(3)	Ag(2)-N(5)	2.27(5)
Ag(3)-N(16)	2.12(4)	Ag(3)-N(15)	2.21(4)
Ag(4)-N(3)	2.03(3)	Ag(4)-N(8)	2.07(4)
Ag(5)-N(18)	2.07(6)	Ag(5)-N(14)	2.14(3)
Ag(6)-N(9)	2.12(4)	Ag(6)-N(13)	2.12(4)
Ag(7)-N(20)	2.09(4)	Ag(7)-N(26)	2.14(3)
Ag(8)-N(11)	2.10(4)	Ag(8)-N(21)#4	2.19(4)
Ag(9)-N(6)	2.11(3)	Ag(9)-N(2)	2.11(3)
Ag(10)-N(24)	2.10(3)	Ag(10)-N(1)	2.10(4)
Ag(11)-N(12)	2.10(4)	Ag(11)-N(4)	2.17(4)
Ag(12)-N(19)	2.14(3)	Ag(12)-N(23)	2.16(3)
Ag(13)-N(17)	2.13(4)	Ag(14)-N(10)	2.14(3)
Ag(15)-N(22)	2.08(4)	Ag(15)-N(25)#3	2.11(3)
Ag(1)-O(3)#3	2.57(2)	Ag(2)-O(4W)	2.25(5)
Ag(2)-O(5)	2.56(3)	Ag(3)-O(43)	2.60(3)
Ag(5)-O(48)	2.56(3)	Ag(12)-O(49)#3	2.60(3)
Ag(14)-O(1W)	2.491(18)	Ag(15)-O(41)#6	2.53(3)
Ag(16)-O(2W)	2.40(4)	Ag(16)-O(31)	2.54(2)
N(14)-N(25)-Ag(15)#1	123(2)	N(7)-Ag(1)-N(27)#2	164.1(11)
N(7)-Ag(1)-O(3)#3	106.8(10)	N(27)#2-Ag(1)-O(3)#3	85.2(9)
N(16)-Ag(3)-N(15)	167.2(12)	N(16)-Ag(3)-O(43)	87.2(13)
N(15)-Ag(3)-O(43)	85.5(12)	N(3)-Ag(4)-N(8)	174.9(15)
N(18)-Ag(5)-N(14)	156.0(18)	N(18)-Ag(5)-O(48)	103.7(18)
N(14)-Ag(5)-O(48)	80.4(11)	N(9)-Ag(6)-N(13)	170.4(15)
N(20)-Ag(7)-N(26)	173.0(16)	N(11)-Ag(8)-N(21)#4	165.6(14)
N(6)-Ag(9)-N(2)	156.2(13)	N(24)-Ag(10)-N(1)	171.7(15)
N(12)-Ag(11)-N(4)	160.1(13)	N(19)-Ag(12)-N(23)	174.2(14)
N(19)-Ag(12)-O(49)#3	80.7(12)	N(23)-Ag(12)-O(49)#3	93.5(11)

Symmetry transformations used to generate equivalent atoms: #1 = -x+2,y+1/2,-z+1/2; #2 =x,-y+1/2,z-1/2; #3 = -x+2,y-1/2,-z+1/2; #4 = -x+2,-y+1,-z+1; #5 =x,-y+1/2,z+1/2; #6 = -x+1,y-1/2,-z+1/2; #7= -x+1,y+1/2,-z+1/2.

References

1 G. M. Sheldrick, *SADABS; ver. 2.10*; University of Gottingen: Göttingen, Germany, 2003.
2 G. M. Sheldrick, *SHELX-97, Program for Crystal Structure Refinement*, University of Göttingen: Germany, 1997.
3 J. J. Chen, M. D. Symes, S. C. Fan, M. S. Zheng, H. N. Miras, Q. F. Dong and L. Cronin, *Adv. Mater.*, 2015, **27**, 4649-4654